HAL
open science

# Global RC Structural Damage Index based on The Assessment of Local Material Damages

Sofiane Amziane, Jean-François Dubé

## To cite this version:

Sofiane Amziane, Jean-François Dubé. Global RC Structural Damage Index based on The Assessment of Local Material Damages. Journal of Advanced Concrete Technology, 2008, 6 (3), pp.459-468. 10.3151/jact.6.459 . hal-00359415

**HAL Id: hal-00359415**

**https://hal.science/hal-00359415v1**

Submitted on 10 Aug 2009

**HAL** is a multi-disciplinary open access archive for the deposit and dissemination of scientific research documents, whether they are published or not. The documents may come from teaching and research institutions in France or abroad, or from public or private research centers.

L'archive ouverte pluridisciplinaire **HAL**, est destinée au dépôt et à la diffusion de documents scientifiques de niveau recherche, publiés ou non, émanant des établissements d'enseignement et de recherche français ou étrangers, des laboratoires publics ou privés.

# Global RC Structural Damage Index based on The Assesment of Local Material Damages

**Sofiane Amziane, Jean Francois Dubé**

*Professor at Polytech'Clermont-Ferrand, Departement of civil Engineering Université Blaise Pascal, BP 206, 63174 Aubière Cedex, France*
*Sofiane.Amziane@polytech.univ-bpclermont.fr*

*Professor at Université Montpellier II, LMGC - UMR 5508 CNRS-U*
dube@lmgc.univ-montp2.fr

*ABSTRACT. This study presents a computational method to estimate a global damage index of a RC construction. The method is based on the evaluation of local damages combined to an analysis of the probable collapse mechanism of the structure. A constitutive model for reinforced concrete, including global damage variables for concrete and steel elasto-plastic models, is integrated in a multilayered finite element code. So, the location of pseudo plastic hinges in a structure is obtained in the areas of maximal damage, resulting from the simulation by FE method. The global index is derived from a specific formula taking into account the damage recorded in the critical zones of the structure (pseudo plastic hinges) and the damages computed in the less damaged areas.*
*The proposed method is validated on a RC frame structure application. The diagram "global index vs. loading" has shown a specific shape and gives interesting results to discuss the possibility of reparation.*

**Keywords** *: local damage, global damage, index damage, concrete, steel, numerical simulation, frame, limit analysis*

***Nomenclature:***

| | |
|---|---|
| $D_n$ : local damage following $\vec{n}$ direction<br>$D_c(u)$ : compressive damage of a layer with *du* thickness<br>$D_c$ : averaged compressive damage of a concrete cross section<br>$D_{cl_i}$ : compressive damage of each "i th" layer in the case of multilayered finite element discretization<br>$D_{tl_i}$ : steel tensile damage of each "i th" tensile layer in the case of multilayered finite element discretization<br>$D_{c_{peak}}$ : concrete compression damage corresponding to the strain at peak stress<br>$D_{compression}$ : averaged compression damage of the element<br>$D_{traction}$ : averaged tensile damage of the element<br>$D_{element}$ : damage of the element<br>$D_i$ : Damage of i th element pseudo-hinge in progress (section with the higher amount of damage)<br>$D_j$ : Damage of j th element of the other damaged cross-section<br>$D^-_{global}$ : global damage for negative displacement<br>$D^+_{global}$ *: global damage* for positive displacement<br>$D_{global}$ : global damage index (damage of the structure)<br>$p$ : number of non-dependent collapse mechanisms<br>$m$ : the number of critical cross sections (plastic hinge)<br>$h$ : degree of indeterminacy | $S$ : cross area<br>$\vec{n}$ : normal to the element<br>$S_D$ : damaged section<br>$u$ : depth of the neutral axis;<br>$Y$ : total length of the compressed zone;<br>$b(u)$ : width of the section relatively to the ordinate $u$;<br>$S_c$ : compressed area;<br>$S_t$ : area in tension;<br>$S_c(Y)$ : compressed area relatively to the position $Y$<br>$E_{0.4}$ : Young modulus defined at 0.4 $f_c$ stress<br>$E_{ir}$ : initial reloading modulus<br>$f_c$ : peak stress in MPa<br>$\varepsilon_r$ : residual strain<br>$\varepsilon_f$ : failure strain<br>$\varepsilon_0$ : strain at the peak stress<br>$\varepsilon_p$ : plastic strain<br>$\varepsilon_e$ : maximal elastic strain<br>$\varepsilon_{max}$ : maximal plastic strain |

## 1. Introduction

The reinforced concrete damage index allows for the assessment of the damage of a section (local scale, e.g. material), an element (intermediate scale, e.g. a beam or a column) or a structure (global scale, e.g. a building), relatively to the ultimate resistance of the considered scale.

At the local scale, damage can be approached by the evaluation of material damage through the behavior model and through the framework of the mechanics of damage. This approach is well adapted to the use of numerical methods such as FEM [1,2] and allows for the acquiring of damage diagrams of structures.

The local indices may involve a single damage parameter such as maximum deformation (curvature, rotation) or dissipated energy, or two or more parameters [3]. In the literature, there are a number of damage indices which use criteria such as the ductility [4,5 and 6], the inflexibility [7], the dissipated energy [8] including the number of cycle loadings [9].

At a global scale, the damage index evaluation of a RC structure is often based on the concept of these indicators. These indices analyze how the structures respond to monotonous and/or cyclical demands. In addition to the techniques cited for the local damages, global index damages analyze the flexural bending-curvature, strength-displacement, stiffness and strength degradation responses of the structure [10].

A detailed study of these indicators integrating a larger state of the art about the different classification of the damage indices including deterministic and probabilistic approaches has been presented by Kappos [3]. Also, it can be noted the classification of [11] who state that the response-based damage indices can be divided into three groups according to what the index stands for:

1) maximum deformation (such as ductility ratio, interstorey drift, slope ratio, flexural damage ratio, maximum permanent drift);

2) cumulative damage (such as normalized cumulative rotation, low cycle fatigue);

3) maximum deformation and cumulative damage such as Park and Ang's local damage index [5], Maximum softening, final softening and Chung et al. Local damage index [12].

Whatever the complexity, the local or global approach of damage can be an efficient tool for the decision-maker compelled to choose between repairing, reinforcing or destroying the structure.

However, two questions reside for a given structure and load:

- what is the link between the damage diagram provided by the local approach, and the global damage given by an indicator?
- how should the indicator value be interpreted to be able to take the repair or the destroy decision?

The aim of this paper is to present a method able to evaluate the global damage of a structure from its local damage of concrete and reinforcement. This gives a damage index using the advantages of both levels of approaches: localization of damage and global synthesis.

In the literature, using a 3D elasto-plastic and fracturing model for normal strength concrete Tsuchiya and Maekawa [13] have proposed with success a similar aproach based first on the calculus of the average of local damage deduced from the concrete model, which are integrated then to the whole structure. The application of this approach is combined here to the plastic analysis of the stability of structures.

## 2. Methods

There are two main steps in the proposed method:

- Simulation of the structural behavior using FEM. Concrete and Steel model behavior is adapted to our problem and allows us to ascertain local damage;
- Analysis of the simulation results and calculus of the global damage.

The link between these two steps uses the failure mechanism concept which is directly linked to the local analysis of the structure. A mechanism results from the appearance of a zone where either distortion, or curve, is extreme. These zones are characterized by important amounts of concrete deterioration and/or by an extreme plastic distortion of steel reinforcement in tension [14]. For concrete this zone is a pseudo-plastic hinge (points 1, 2 and 3 in Figure 1).

The zones where plastic hinges appear are considered as critical sections; they correspond for example to the points of structure where the bending moment can introduce an extremum: support or loading position (points 1, 2 and 3 in Figure 1).

To assess the total damage resulting from the represented mechanism, the proposed method requires four stages:

- Finite element numerical simulation gives the local damages to evaluate the element degradation (damage of each cross section),
- location of the critical sections (extrema of damage),
- determination of the probable failure mechanism,
- total damage computing, relating the failure mechanism progress.

This computing process is applied to every time or loading step in the static and cyclical case.

## 3. Evaluation of local damage

A section of reinforced concrete can be easily modeled as a stack of several layers of steel and concrete. The multilayer finite element has therefore been selected for this study to be able to assess local damage [15].

The first step is to compute cross section damage including the calculus of compression and tensile damage in concrete and steel, respectively.

The collapse of a reinforced concrete beam submitted to a bending loading is commonly the result of the crushing of the compressed concrete with an excessive plastic deformation of steel reinforcement in tension. At this stage of damage, the concrete in tension no longer plays a role and has no effect on the level of resistance of the cross section. The concrete is completely cracked and is therefore unable to transmit any strength.

These two important observations allow us to define the FE ruin if one of the following conditions appears:

- ruin of the element by concrete crushing due to the compression stress,
- ruin of the FE due to excessive plastic deformation of steel.

### 3.1 *Damage of compressed concrete*

Considering a damaged solid volume (Figure 2), $S$ the cross area where $\vec{n}$ is normal to the element and $S_D$ the damaged section, Lemaitre and Chaboche [16] has defined the local damage following $\vec{n}$ direction by the variable $D_n$ as:

$$D_n = \frac{S_D}{S} \qquad (1)$$

with $D_n = 0$ for the material without damage, $D_n$ is comprised between 0 and 1 for the damaged material and $D_n$ equal to 1, at the ruin following the direction $\vec{n}$.

The damage model is used to compute stresses following:

$$\sigma = E_0 (1 - D_c)\varepsilon(u) \qquad (2)$$

Where $\sigma$ is compressed stress, $E_0$ the Young modulus and $\varepsilon(u)$ is the strain.

The average of compressive damage $D_c$ of a cross section (Figure 3) is defined by :

$$D_c = \frac{1}{S_c}\int_0^Y D_c(u)\cdot dS_c(u) \qquad (3)$$

$$dS_c(u) = b(u)\times du \qquad (4)$$

$D_c(u)$ is the compressive damage of a layer with $du$ thickness, $u$ is the depth of the neutral axis, $Y$ *is* the total length of the compressed zone, $b(u)$ is the width of the section relatively to the ordinate $u$, $S_c$ is the compressed area, $S_t$ is the area in tension.

When $u=Y$, $S_c(Y)$ is the compressed area relatively to the position $Y$ and $S_c = S_c(Y)$.

In the case of pure compression $D_c=D_c(u)$. In flexion $D_c<D_{cmax}(u)$. In fact, the damage influence of extreme fibres is minimized to keep only, one average damage.

To describe the concrete damage, the Young modulus evolution according to the material strain criterion is used. This evolution is deducted from the application of loading cycles. The slope $E_{ir}$ at the origin of the diagram (Figure 4) is then calculated. An empiric law described in [18] allowed us to write the evolution of the ratio $\frac{E_{ir}}{E_{0.4}}$ according to $f_c$ and of $\frac{\varepsilon_r}{\varepsilon_0}$ as:

$$\frac{E_{ir}}{E_{0.4}} = \frac{1}{\mu\left(f_c, \frac{\varepsilon_r}{\varepsilon_0}\right)} \quad \text{and} \quad D_c(u) = 1 - \frac{E_{ir}}{E_{0.4}} = 1 - \frac{1}{\mu\left(f_c, \frac{\varepsilon_r}{\varepsilon_0}\right)} \qquad (5)$$

Where: $\mu\left(f_c, \frac{\varepsilon_r}{\varepsilon_0}\right) = 1 + (4.2 - 0.034 \times f_c) \times \left(\frac{\varepsilon_r}{\varepsilon_0}\right)$ (6)

The damage parameter $D_c(u)$ (equation 3) defines the local damage evolution of concrete (Figure 5), according to the residual strain rate. The residual strain variation is experimentally identified as:

$$\frac{\varepsilon_r}{\varepsilon_0} = \left(2.7 \times 10^{-3} \times f_c - 0.01\right) \times \left(\frac{\varepsilon}{\varepsilon_0}\right)^{(2+0.02 \times f_c)} \quad (7)$$

where $f_c$ is the peak stress in MPa, $\varepsilon_r$ is the residual strain, $\varepsilon_0$ is the strain at the peak stress, $E_{ir}$ is the initial reloading modulus and $E_{0.4}$ is theYoung modulus defined at 0.4 $f_c$ stress

3.2 ***Local damage of section in tension***

In the cross section in tension, the concrete is neglected. Tensile strength of concrete is very weak (not higher than 4 MPa), then only the steel plasticity is taken into account to evaluate the damage of the zone in tension following equation 8 [16] :

$$D_t = \frac{\varepsilon_p}{\varepsilon_{\max} - \varepsilon_e} \quad (8)$$

Where $\varepsilon_p$ is the plastic strain and $\varepsilon_e$ is the maximal elastic strain (figure 6). The $\varepsilon_{max}$ strain is fixed at 1 %. This value can be changed by more precise experimental results.

The concept of excessive strain of the reinforcements assumes that the definition of an acceptable maximum strain $\varepsilon_{max}$, translating an absolute limit of deformation of steels. The conventional value for the ultimate limiting states $\varepsilon_{max}$ = 1 % in European Building Codes has been adopted.

This indicator gives the evolution of the plastic hinge. The damage defined as the variation of the elastic slope only starts progressing at $\varepsilon_e$=0.25%. This relation states that the indicator is null until $\varepsilon$=$\varepsilon_e$ and 1 for $\varepsilon$ = 1 % (Figure 6).

### 3.3 ***Semi Local Damage in the multilayered discretization case***

In the case of the finite element method, the real structure is usually modeled as a plane structure including beams and columns.

In order to take into account the location of the steel reinforcement, a multilayer discretization is adopted. For this reason, the EfiCos code is used [15,17].

For each time-step simulation, the constitutive models of concrete and steel are integrated in the FE code and gives both, compressive concrete damage for each layer and tensile "pseudo-damage" of steel for the steel layers, (Figure 7).

The damage of the layers $D_{c_{l_i}}$ represents the local damage which shows degradation at the elementary volume scale. It's computed using equation 3 adapted to the layer geometry.

The collapse of the element by compression is obtained when the peak stress of concrete is reached (Figure 8). Consequently, the compressive concrete damage of the "i th" layer $D_{c_{l_i}}$ is dimensionless:

$$\overline{D_{c_{l_i}}} = \frac{D_{c_{l_i}}}{D_{c_{peak}}} \xrightarrow[\varepsilon \to \varepsilon_0]{} 1 \qquad (9)$$

Where $D_{c_{peak}}$ is the concrete compression damage corresponding to the strain at peak stress on figure 5.

This formula verifies : $\overline{D_{c_{l_i}}}$ =1 at the peak stress, $\overline{D_{c_{l_i}}}$ <1 before the peak and $\overline{D_{c_{l_i}}}$ >1 after the peak.

The average of the $\overline{D_{c_{l_i}}}$ local damage gives the value of the compressive damage of the element and is noted (Figure 9): $D_{compression}$ computed with the equation 11:

$$D_{compression} = Min\left( \frac{\sum_i D_{c_{l\,i}} S_i}{\sum_i S_i} ;1 \right) \qquad (10)$$

In compression we supposed that the ruin is obtained with the peak of behavior. In flexion the average damage does not exceed one.

With the same concept, the damage of the steel layers can be averaged out. The steel tensile damage $D_{traction}$ is then obtained.

Finally, the element damage is the maximum between tensile damage and compressive damage:

$$D_{element} = \text{Max}\ (D_{compression}\ ,\ D_{traction}) \qquad (11)$$

With this definition, the ultimate damage is obtained when:

$D_{compression}$ = 1 inducing the collapse of compressed concrete or $D_{traction}$ = 1 which indicate the excessive strain of steel reinforcement.

## 4. Global damage concept

### 4.1 *Failure mechanism*

The concept presented by [19] has been adopted to define the ruin mechanism of structures composed of straight bended beam. Essentially, the failure mechanism depends on the value $p$ which is the number of non-dependent ruin mechanisms following:

$$p=m-h \qquad (12)$$

Where "m" is the number of critical cross sections and $h$ is the degree of indeterminacy.

The critical zones "m number" where plastic hinges can appear are located at each loading increment or time step of the simulation result. The probable failure mechanism is then easily predicted. The critical zones are where the damage material is extremal (at the connection, in the middle of the beam, at the loading points, at the cross-section changes).

When the number of non-dependent ruin mechanisms “p” is negative or is equal to 0 the stability of the structure is guaranteed. The instability of the structure is observed if “p” exceed zero.

4.2 ***Global damage assessment in the static case***

The global damage of a structure is designed respecting the four following conditions:

- Taking into account of whole damaging zones of the structures;
- Presence of zones other than the most critical zones (plastic hinges) inducing the collapse are taken into account. These zones increase the level of global damage;
- The whole critical section must have the same weight in the definition of the global damage;
- The global damage must reach the value 1 (100 %) at the ruin and collapse.

From these criteria, the proposed global damage is:

$$D_{global} = \frac{\sum_{i=1}^{m} D_i + \sum_j D_j}{m + \sum_j D_j} \qquad (13)$$

$i$ : i th element pseudo-hinge in progress (section with the higher amount of damage)

$j$ : j th element of the other damaged cross-section

m : number of critical cross sections

The proposed global damage index checks the stated requirement:

- All types of damages are taken into account with the same weight (addition of the damages)
- Global damage equal to 1 when the structure failed:

$$\sum_{i=1}^{m} D_i = m \Rightarrow D_{global} = \frac{m + \sum D_j}{m + \sum D_j} = 1 \qquad (14)$$

Moreover, it can be noted that the $D_{global}$ value equal to 1 corresponds precisely to the changing state of the structure which becoming instable (p > 0).

### 4.3 *Global damage assessment in the cyclic and dynamic case*

In the cyclic or seismic case, alternative global damage depending on the direction of the displacement or loading should be assessed:

- $D^{+}_{global}$ for positive displacement
- $D^{-}_{global}$ for negative displacement

The global damage is then taken as the maximum of the two values so that the damage always increases (degradation is irreversible).

$$D_{global} = Max\left(D^{-}_{global}, D^{+}_{global}\right) \tag{15}$$

## 5. Numerical implementation

The constitutive model for steel and concrete presented in part 3.1 has been implemented in the EFiCoS code [15,17]. ANALYDA (ANALYse of DAmmage), a program able to compute the global index damage, has been developed using the FE results of EFiCoS.

### 5.1 *Numerical tool "EFiCoS"*

To perform non-linear simulation, the code uses 2D beam elements with multilayered fibers (Figure 10). The basic assumption is that plane sections remain plane (Bernoulli's kinematic) allowing to consider a uniaxial behavior of each layer. The static, cyclic or seismic loadings are considered as input data. The code combines the advantage of using structural elements with the simplicity of true uniaxial behavior or enhanced uniaxial behavior including shear [13].

An element includes concrete and/or steel layers. A perfect bond between each layer is assumed. The concrete and steel strain is assumed equal in the layer containing steel and concrete.

## 6. Application

As an application example consider the case of the one storey reinforced-concrete frame shown in Figure 11 [20]. Masses are applied in top of column (50kN) and on the beam (3x15kN) to represent the static loads. One lateral displacement is applied at the node two to represent the seismic effect. This force is static monotonous or cyclic. The cross-section dimensions and steel reinforcement for the beam and columns are also shown in Figure 11. The frame is fitted at its base and presented a multi-plastic hinge when failed.

The structure tested by CEBTP [20] has a rectangular shape (1.831×1.5525 m). Both columns have the same cross sections (0.135×0.135 m) and the beam has a (0.235×0.135 m) cross section. The maximal compressive strength of concrete was 33 MPa and the yield elastic stress of steel was 475 MPa.

The cross section of the frame is discretized in ten layers (including two steel ones), and the structure in 58 elements and 59 nodes.

Figure 12 shows the failure mechanism of the frame which is due to the plastic-hinge formation at the base and the top of each column and at the corner of the frame.

### 6.1 *Static monotonous simulation*

Figure 13 shows the monotonous static response in terms of load and lateral displacement at the beam level. There is a good correlation between the experiment and the numerical simulation. The report of test specifies that the collapse of the structure by instability was obtained for a top displacement and an ultimate force of 35 mm and 33 kN, respectively. At this ultimate stage, the

concrete presented a dramatic cracking pattern at the base and the top of the two columns, the steel reinforcement was strongly plasticized. The top frame continued to move without possible stabilization following a panel mechanism which defines this collapse.

.

### 6.2 *Cyclic simulation*

For the cycling loading test, two hydraulic actuators are used in order to move the top columns alternatively on both sides with symmetry plane.

Figure 18 shows a good correlation between the experimental response of the frame and the simulated load – displacement diagram for the large displacements. The area of each cyclic curve has also been correctly simulated which demonstrates the robustness of the concrete and steel model behaviors and the finite element used to quite accurately represent the damage and damping occurring for this loading case.

## 7. Damage Analysis

The damage analysis was conducted in three steps: 1) Static and cyclic simulation of global response of the studied structure (see below), 2) Computing of local damage materials (concrete $D_{c_{li}}$ and steel $D_t$), 3) Location of the critical sections inducing the collapse, 4) The global damage index is computed using the proposed approach as given by equations (13, 14, 15).

### 7.1 *Local damage: monotonious case*

The main goal of the local approach is to obtain the stress and strain diagram of the frame. The computed values are used to evaluate the local damage with equations (3 and 8).

(Figure 16.a) and (Figure 16.b) shows the compressive and tensile damage diagram of concrete for a displacement of 30 mm, which represents 90% of the ultimate lateral displacement.

These charts confirm the experimental results for the localization of the critical sections and major degradations. From the major to the minor, the strain and stress are maximal in sections 3, 4, 1 and 2, respectively.

The higher levels of the plastic strain of the steel reinforcements are located at these positions. Compared to these critical sections, the analysis of the results shows that the damage to the beam is negligible (less than 1%). Then, the probable mechanism determined by ANALYDA is a panel mechanism containing pseudo plastic-hinge 1, 2, 3 and 4.

#### 7.1.1 *Steel reinforcement in tension and compressed concrete damages*

The plasticity criterion adopted (equation 8) states that the damage is null as long as steel is elastic. The damage increases linearly from 0% to 100%. 100% is reached when the plasticity is equal to a strain limit conventionally chosen at 1%. Consequently, the damage evolution of steel presented in Figure 15 is linear for the four critical sections.

Compared to the total damage of the structure, it can be noted that for displacements lower than 13 mm, i.e. before steel plasticity, all of the damage comes from the degradation of the concrete (Figure 14 and point A in Figure 15). For displacement higher than 13 mm, global damage results from both compressive damage (Figure 14) and plasticity of the steel reinforcement (Figure 15). In a first phase, sections 3 and 4 undergo a plastification and thereafter the two other sections (1 and 2): then their damage increases much more quickly starting from 16 mm for section 1 and 26 mm for section 2; plasticity of steel leads to the emergence of pseudo-hinge for 30 mm lateral

displacement. The last pseudo-hinge emerges in section 2, leading to the collapse of the structure by panel mechanism (Figure 12 at 21 mm).

Each appearance of a pseudo-plastic hinge (Figure 15) is accompanied by light discontinuity (points A, B, C).

### 7.2 *Evolution of the global damage in the frame*

The curve of the total damage takes a regular form, marked by an inflection around 50% of global damage noted C (Figures 17 end 15). Compressive concrete damage of three sections is around 50% and tensile damage exceeds 50% for these sections.

Observation of the curves of the local damages (Figures 14 and 15) revealed that the point of inflection corresponds precisely to the creation of the last pseudo plastic hinge in section 2. From this critical state (22 mm of displacement, Figure 15), the damage evolves by excessive deformation of the reinforcements, until the nearly simultaneous formation of the first pseudo-hinge (sections 3, 4, 1) to 25 mm of displacement. Starting from 30 mm of displacement, a logical deceleration of the damage can be observed since the only damage which continues to evolve is that of section 2 (the other sections degenerated into pseudo-hinge).

Finally, the collapse of the framework following our criteria occurs for a displacement of 38 mm, for a real ruin to 35 mm (Table 1). The prediction of the ruin is satisfactory.

Following the simulated results and the analysis proposed by Tichy and Rakosnik [14], a decision tool allowing us to choose betwen the possibility of repairing or destroying the structure leads to:

- before the inflection point (point C in figure 17): we can repair and reinforce the structure,

- after the inflection point: we can envisage to destroy the structure.

After the inflection point, all critical sections are plasticized and present an important and irreversible strain. These deformations are dangerous because of the possibility of sudden collapse. It is probably safer and costly to destroy the structure than to repair it.

After the inflection point, all the critical sections are plasticized and present an important and irreversible strain. These deformations are dangerous because of the possibility of sudden collapse.

Table 1: Evolution of the damage according to the observation experiment.

| **Displacement** | **Observations** | **$D_{global}$ (%)** |
|---|---|---|
| **[0 – 10] mm** | Tensile damage of concrete | **0-10** |
| **[10 – 20] mm** | Compressive damage of concrete | **10-40** |
| **[20 – 38] mm** | Plastic damage of steel (limit to plan a reparation at Dglobal=50%) | **40-100** |
| 28 mm | Plastic hinge 3 appears. | 82 |
| 29 mm | Plastic hinge 4 appears. | 86 |
| 30 mm | Plastic hinge 1 appears. | 89 |
| 38 mm | Plastic hinge 2 appears. Structure collapses due to a mechanism with 4 hinges | 100 |

7.3 ***Global damage in the cyclic case***

The simulation of evolution of the total damage is presented in Figure 19. The distribution of the damage is a function of the number and the amplitude of the cycles. The collapse (global damage = 100%) is recorded at 30 mm displacement at the end of the last cycle. In comparison with the static damage, the cyclic one induces more degradation in the structure. This observation confirms the experimental data.

## 8. CONCLUSION

The principal objective of this study is to show the connection between the various levels of the damage approaches relating to the degradation of the structures. Theoretical background shows that there are two principal types of approaches: local approach and global solution coupled to index damage. Each one of these two forms of approaches is confined to an observation level, either local, or global.

The proposed method allows us to make a link between the local damage and the global damage letting us to preserve the advantages of the two approaches. The method suggested was developed around the concept of ruin mechanism and the concepts of the plastic design of the structures.

The performance of the proposed global damage index is illustrated on an RC frame which was tested under monotonious and cyclic lateral loading. The model fit and predictions in terms of local damage locations, degradation progress and structure collapse correspond very well to the ones recorded during the experiments. This is primarily due to the formulation of the global index combining terms describing damage due to each mechanism.

Research in progress includes the calibration of the decision tool and study of the damage on specimens submitted to combined shear and flexure.

**Knowledgements**

The authors gratefully acknowledge Francois DAUBET (Engineer of Ecole Centrale de Nantes) for his intensive contribution on this study. We also would like to extend our thanks to Dr. Jacques LAMIRAULT for his assistance and this approach of the concrete behaviour.

## 9. References


[1] Mazars, J., (1986), "A description of micro- and macroscale damage of concrete structures", *Engineering Fracture Mechanics,* vol. 25, no. 5-6, pp. 729-737.

[2] Mazars J., Ragueneau F., Casaux G., Colombo A. And Kotronis P., (2004), "Numerical modelling for earthquake engineering: the case of lightly RC structural walls", International Journal For Numerical And Analytical Methods In Geomechanics, 28:857-874.

[3] Kappos, A.J., (1997), "Seismic damage indices for R/C buildings: Evaluation of concepts and procedures", Progress in Structural Engineering and Materials, 1(1):78-87.

[4] Banon, H., Biggs, J. M., Irvine, H. M., (1981), "Seismic damage in reinforced concrete frames", Journal of Structural Division. Proceedings of the American Society of Civil Engineers, V. 107, n°ST9, pp 1713-1729, September 1981.

[5] Park Y-J, Ang AH-S & Wen YK., (1987) Damage-limiting aseismic design of buildings. Earthquake Spectra 3( I): 1-25.

[6] Gupta, V., K., Nielsen, S., R., And Kirkegaard, P., (2001), "A preliminary prediction of seismic damage-based degradation in RC structures", earthquake engineering and structural dynamics, vol. 30: pp 981-993.

[7] Lybas, J. M., Sozen, M. A., (1977), "Effect of beam strength and sttifness on dynamic behaviour of reinforced concrete coupled shear walls", Report N°. SRS 444, University of Illinois at Urbana-Champaign.

[8] Meyer, I. F., Kratzig, W. B., Stangenberg, F., Maeskouris, K., (1988), "Damage prediction in reinforced concrete frames under seismic actions", European Earthquake Engineering, vol. 3: pp 9-15.

[9] Sadeghi K., Lamirault J., Sieffert J.G., (1993), Damage indicator improvement applied on R/C structures subjected to cyclic loading. Structural Dynamics- Eurodyn'93, Balkema, Rotterdam, ISBN 90 5410 3361.

[10] Miramontes, D., Merabet, O., and Reynouard, J. M., (1996), "Beam global model for the seismic analysis of RC frames", earthquake engineering and structural dynamics, vol. 25: pp 671-688.

[11] Ghobarah, A., Abou-Elfath, H., and Ashraf, B., (1999), "Response-based damage assessment of structures", Earthquake engineering and structural dynamics, V28-n°1, pp. 79-104.

[12] Chung, Y. S., Meyer, C., and Shinozuka, M., (1987), "Seismic damage assessment of reinforced concrete members", Report NCEER-87-0022, National Center for Earthquake Engineering Research, State University of New York at Buffalo, NY.

[13] Satoshi Tsuchiya and Koichi Maekawa, (2006) "Cross-sectional damage index for RC beam-column members subjected to multi-axial flexure" *Journal of Advanced Concrete Technology*, Vol. 4 No. 1, 179-192.

[14] Tichy, M., and Rakosnik, J., (1977), "Plasticity analysis of concrete frames", Colet's Publishers, LTD.

[15] La Borderie C., Mazars J., and Pijaudier-Cabot G., (1992), "Response of Plain and Reinforced Concrete Structures Under Cyclic Loadings", SP of ACI, V.134, pp 147-172.

[16] Lemaitre J., and Chaboche J.-L., (1994) ,Mechanics of Solid Materials, Cambridge University Press, Cambridge, 556 pp., ISBN 0521477581 09-1994.

[17] Dubé, J.-F., Pijaudier-Cabot, G. & La Borderie, C., (1996), "Rate dependent damage model for concrete in dynamics", Journal of Engineering Mechanics, vol. 122, no. 10, pp. 939-947.

[18] Amziane, S. & Loukili, A., (1999), "Experimental study of static and cyclic behaviour of steel fibre reinforced high performance concrete", Materials and Structures/Materiaux et Constructions, vol. 32, no. 219, pp. 348-353.

[19] Courbon J., (1996), "Plasticité appliquée au calcul des structures", Techniques de l'ingénieur 11-1996, C2050, C2-I Construction – structure, pp.1-10.

[20] Fouré B., (1978), "Essais statiques et dynamiques sur portiques C.E.A", report of Service d'Etude des Structures of CEBTP, Recherche JT, Dossier N°. 912.7.004.

List of Figures:

Figure 1: Failure mechanism in a beam
Figure 2: Illustration of cross section damage
Figure 3: Calculus of the local damage parameter
Figure 4: Typical stress-strain response of concrete under cyclic uniaxial compression
Figure 5: Local damage of concrete under compression according to compressive strength
Figure 6: Plastic damage of steel reinforcement
Figure 7: Multilayered discretization
Figure 8: Dimentioneless damage of concrete under compression
Figure 9: Cross section damage
Figure 10: Discretization by muli-layered beam elements
Figure 11: Geometrical and material characteristics of tested frame
Figure 12: Different types of failure mechanism for a frame
Figure 13: Load-displacement diagram in static case
Figure 14: Top lateral displacement vs compressive damage of the frame
Figure 15: Tension damage versus displacement
Figure 16: Scale and diagram of damage
Figure 17: Global damage versus displacement in static case
Figure 18: Response of the frame: horizontal force on top versus displacement
Figure 19: Global damage according to cyclic lateral displacement in cyclic case

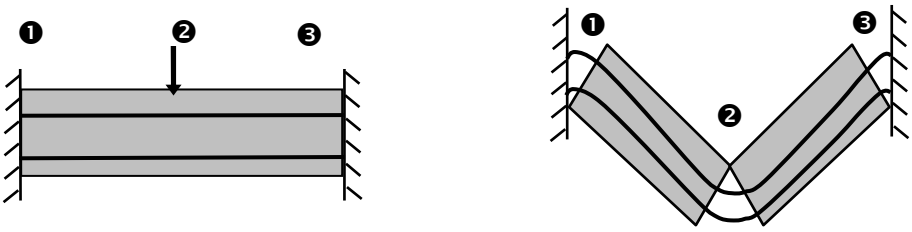


Beam, free from any damage

Collapse of beam due to plastic-hinge formation inducing a failure mechanism

Figure 1: Failure mechanism in a beam

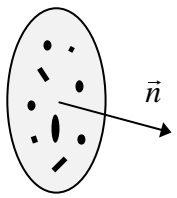


$S_D$ : Lack section (micro-cracks, cavity) characterising the damage of the considered face.

Figure 2: Illustration of cross section damage

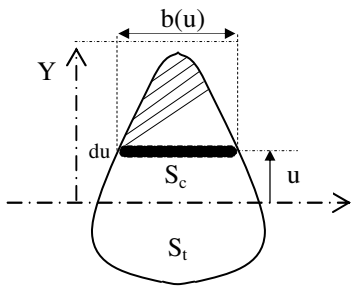


Figure 3: Calculus of local damage principle

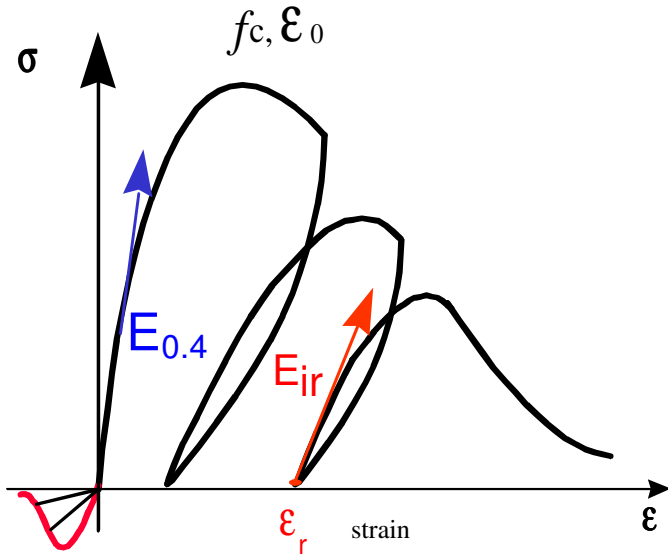


Material models parameter of concrete

Figure 4: Typical stress-strain response of concrete under cyclic uniaxial compression

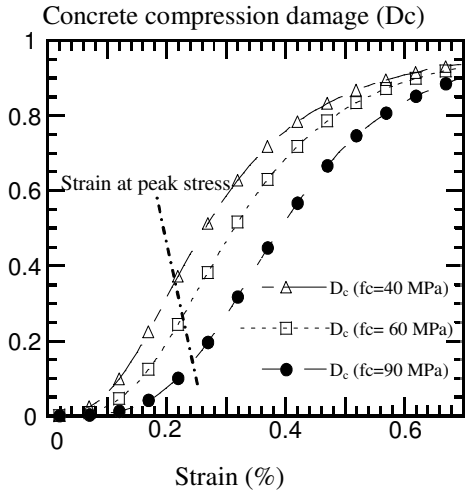


Figure 5: Local damage of concrete under compression according to compressive strength damage at both stress and strain peaks

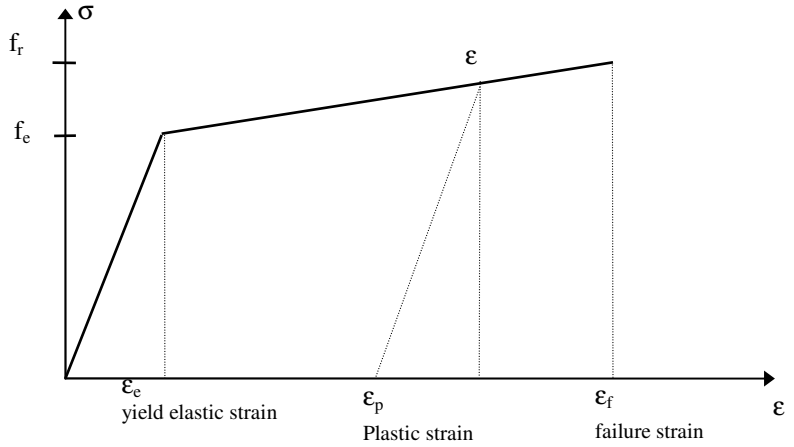


Figure 6: Plastic damage of steel reinforcement

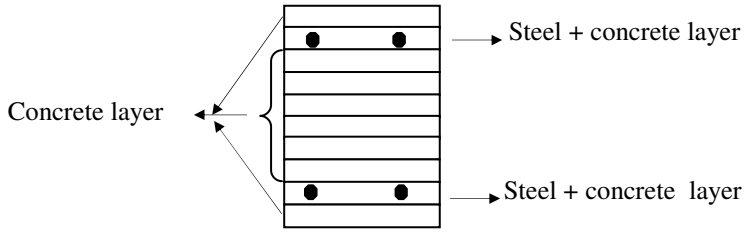


Figure 7: multilayered discretization

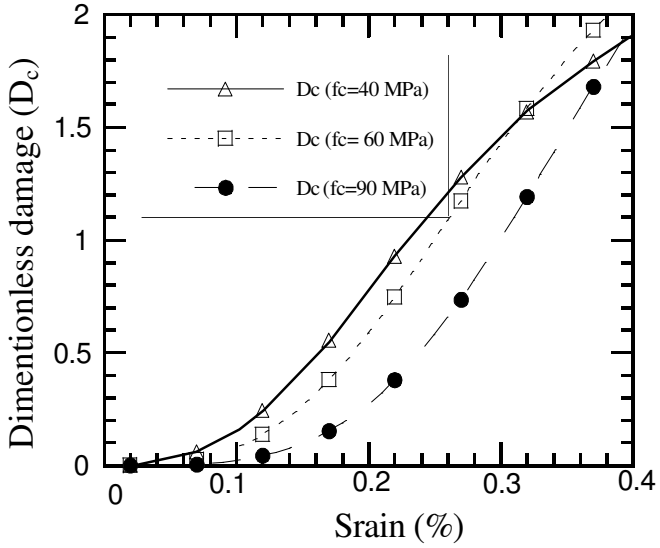


Figure 8: Dimensionless damage of concrete under compression

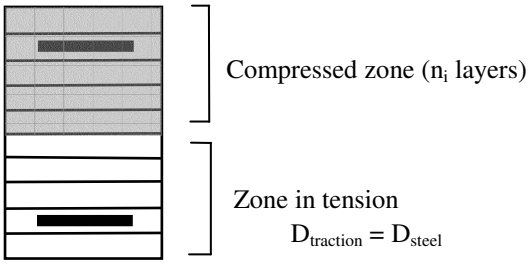


Figure 9: Cross section damage

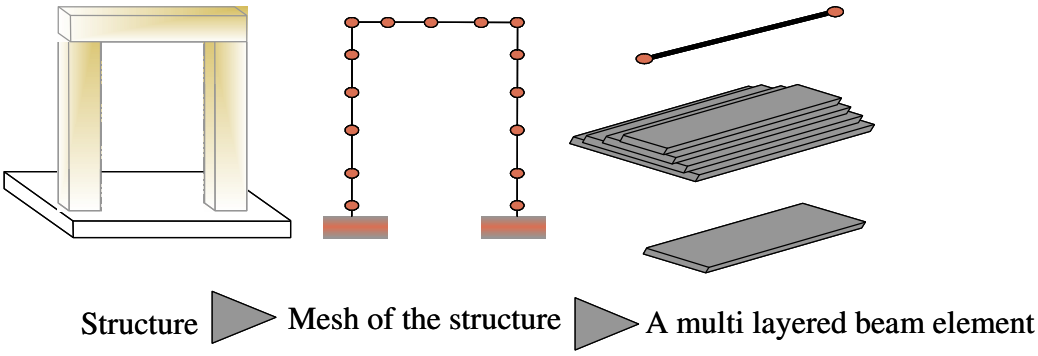


Figure 10: Discretization by muli-layered beam elements

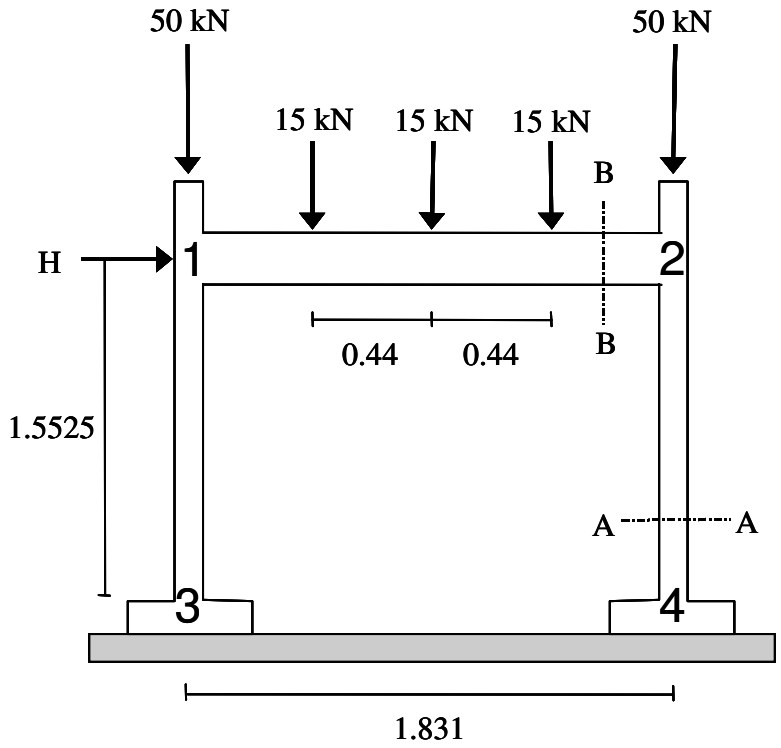


**Materials :**

Concrete : $f_{cj}$ = 33 MPa
$f_{tj}$ = 3.3 MPa
E = 32 500 MPa

Steel : $f_e$ = 475 MPa
E = 213 000 MPa

**Element cross section area :**

A-A : 0.135 x 0.135 (8 T8 + 2T6)
B-B : 0.235 x 0.135 (8 T8 + 4 T6)

**Loading :**

- 145 kN on the beam (2x50 kN + 3x15 kN)
- The H top lateral displacement is applied

Figure 11: Geometrical and material characteristics of tested frame

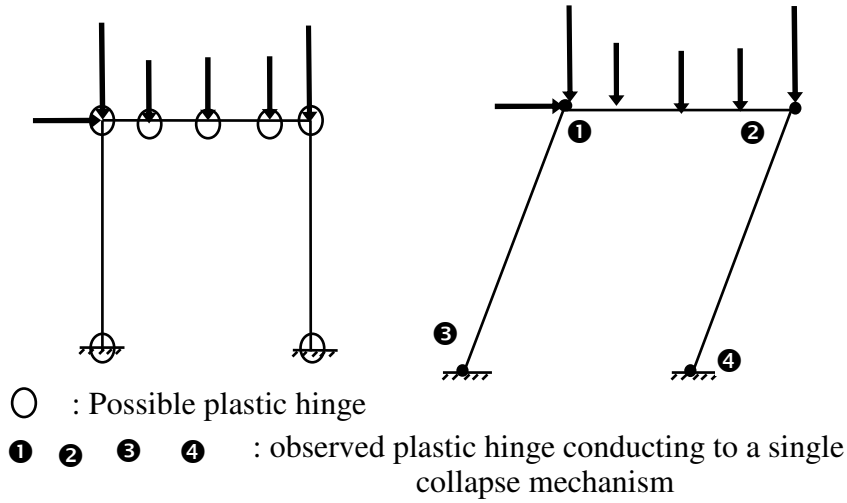


Figure 12: failure mechanism observed for the tested frame

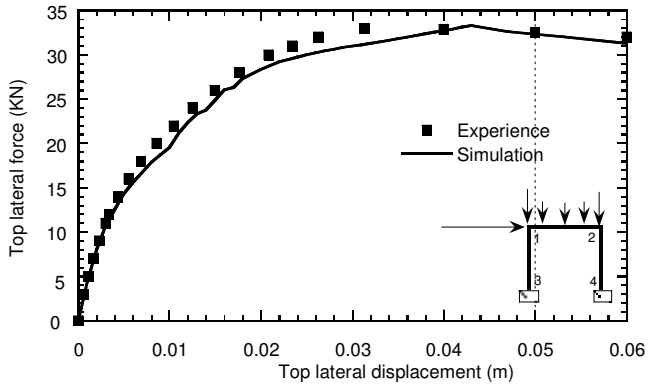


Figure 13: Load-displacement diagram in static case

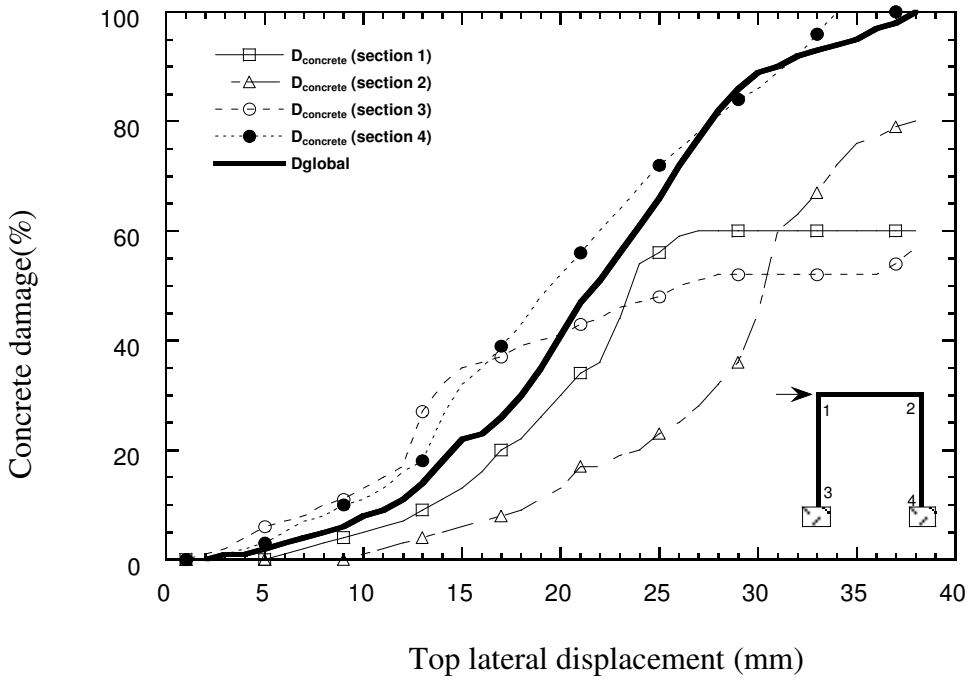


Figure 14: Top lateral displacement vs compressive damage of the frame

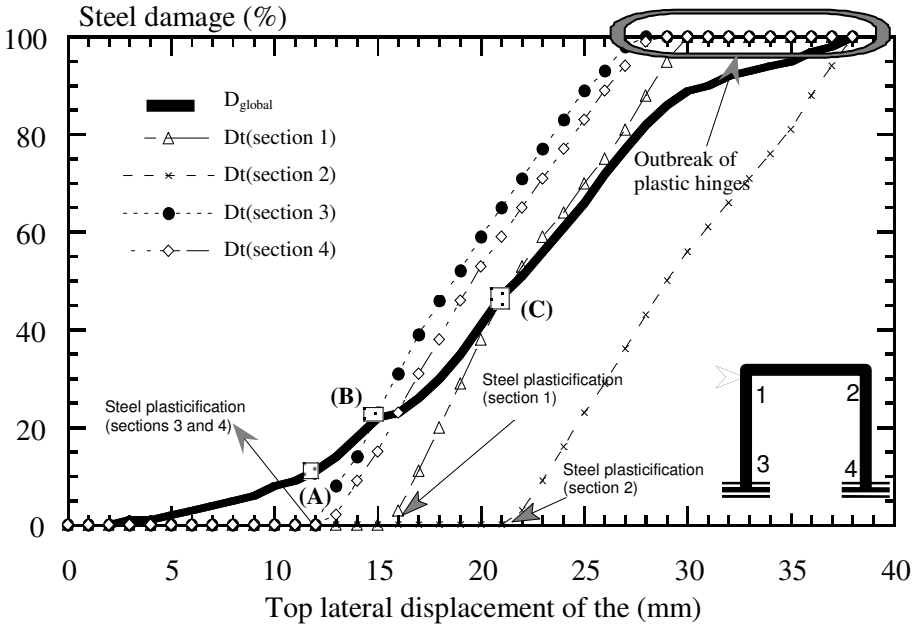


Figure 15: Tension damage (steel damage) versus displacement

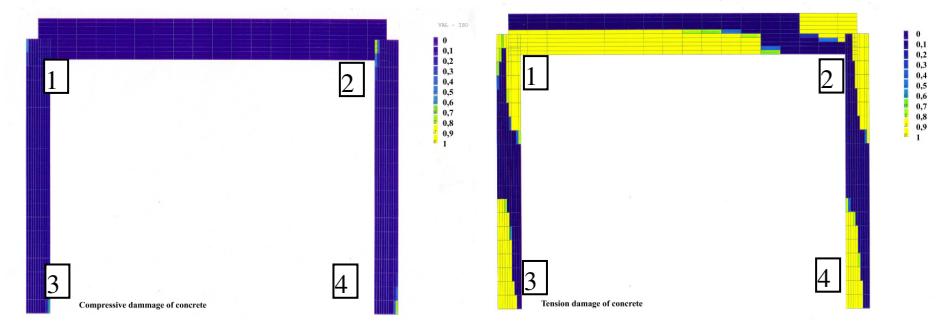


(a) : Compression damage (b) : Tension damage

Figure 16: Scale and diagram damage

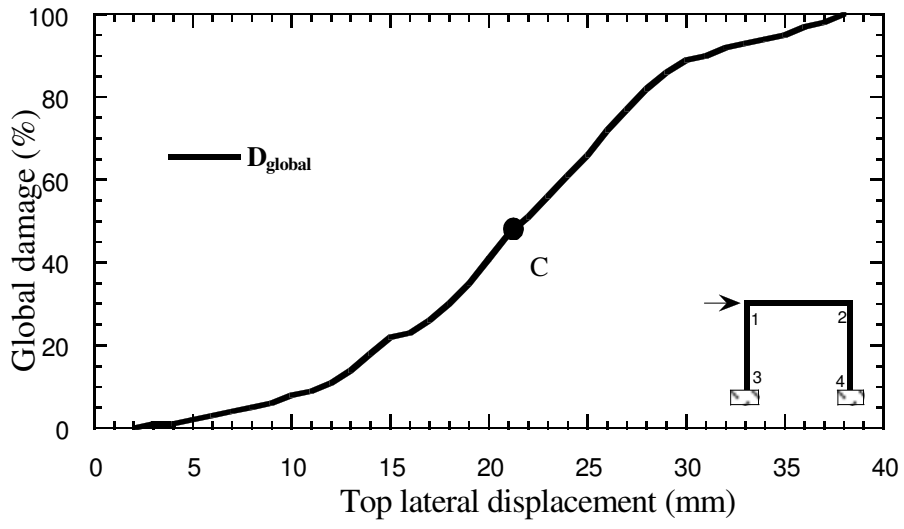


Figure 17: Global damage versus displacement in static case

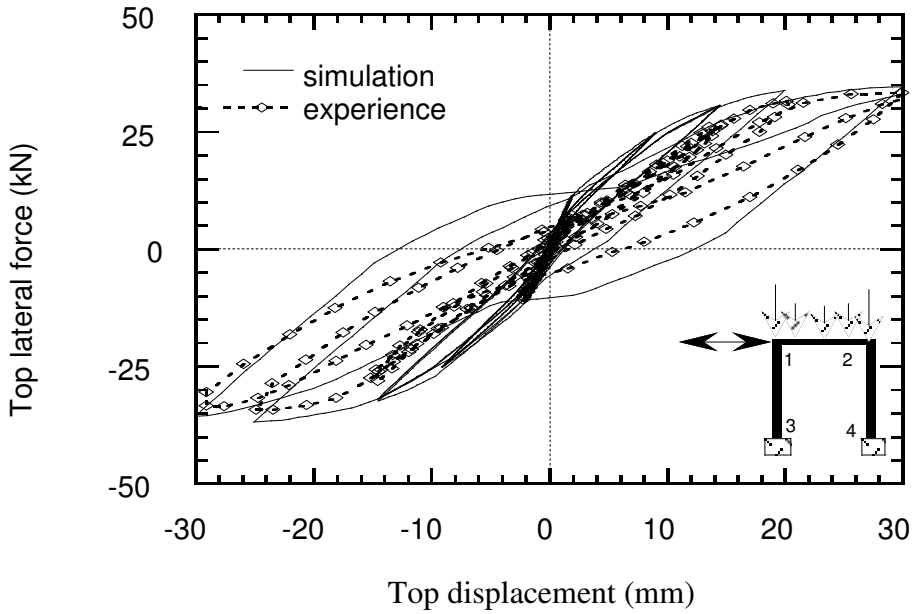


Figure 18: Response of the frame: horizontal force on top versus displacement

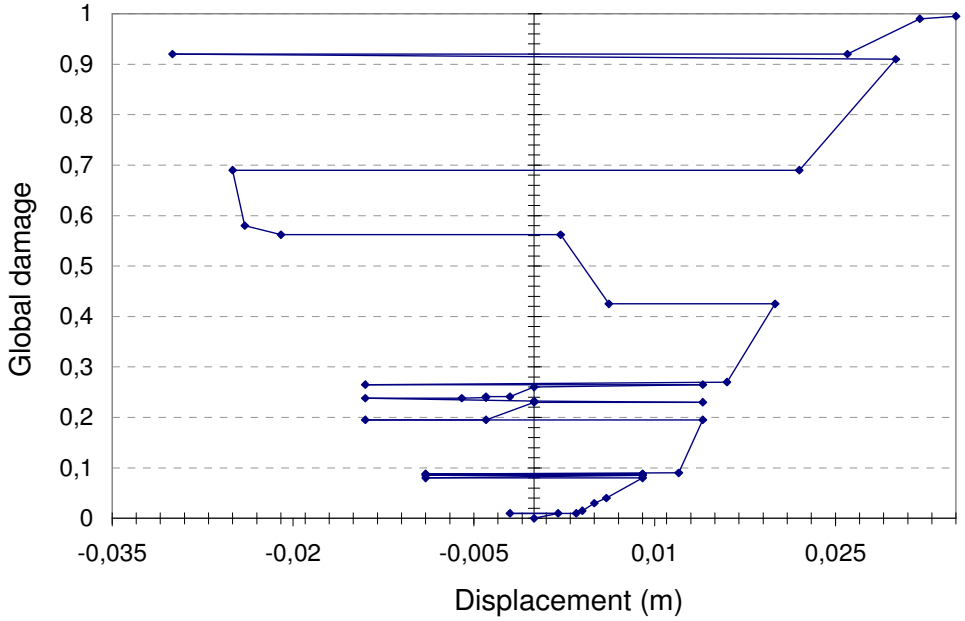


Figure 19: Global damage according to cyclic lateral displacement in cyclic case